



Contents lists available at ScienceDirect

Bioorganic & Medicinal Chemistry Letters

journal homepage: www.elsevier.com/locate/bmcl

Identification of potent and selective MTH1 inhibitors

Alessia Petrocchi^{*}, Elisabetta Leo[†], Naphtali J. Reyna, Matthew M. Hamilton, Xi Shi, Connor A. Parker, Faika Mseeh, Jennifer P. Bardenhagen, Paul Leonard, Jason B. Cross, Sha Huang, Yongying Jiang, Mario Cardozo[‡], Giulio Draetta, Joseph R. Marszalek, Carlo Toniatti, Philip Jones, Richard T. Lewis

Institute for Applied Cancer Science, MD Anderson Cancer Center, 1901 East Road, Houston (TX) 77054, USA

ARTICLE INFO

Article history:

Received 15 January 2016

Revised 9 February 2016

Accepted 10 February 2016

Available online xxxx

Keywords:

MTH1 inhibitors

Antitumor

IACS-4759

2-Aminopyrimidine

ABSTRACT

Structure based design of a novel class of aminopyrimidine MTH1 (MutT homolog 1) inhibitors is described. Optimization led to identification of **IACS-4759** (compound **5**), a sub-nanomolar inhibitor of MTH1 with excellent cell permeability and good metabolic stability in microsomes. This compound robustly inhibited MTH1 activity in cells and proved to be an excellent tool for interrogation of the utility of MTH1 inhibition in the context of oncology.

© 2016 Elsevier Ltd. All rights reserved.

Reactive oxygen species (ROS), such as hydroxyl radical ($\cdot\text{OH}$), hydrogen peroxide (H_2O_2), and superoxide anion ($\cdot\text{O}_2^-$), are cellular metabolism by-products that can react with and damage cellular components like proteins, lipids and DNA. The deoxynucleotide triphosphates (dNTPs) are particularly sensitive to oxidative damage, and incorporation of oxidized nucleotides into DNA can cause mutations and DNA damage.¹ MTH1 (MutT homolog 1) is an enzyme that prevents the incorporation of oxidized purines into DNA by preferentially hydrolyzing 8-oxo-dGTP (8-O-G) and 2-OH-dATP, two of the most abundant oxidative nucleotide lesions, to their corresponding monophosphates.²

In normal cells, ROS levels are tightly controlled in order to maintain intracellular redox homeostasis. On the contrary, altered redox regulation, oxidative stress and increased ROS levels are commonly observed in cancer cells.^{3,4} Recent publications suggest that MTH1 inhibition can specifically kill cancer cells.⁵ It has been proposed that blockade of MTH1 in cancer cells results in abnormally high levels of oxidized bases incorporated into DNA, with a concomitantly increased mutational burden; resulting in genetic instability, and ultimately triggering of cell death mechanisms.^{5,6} Since normal cells have lower ROS levels, MTH1 inhibition would not be expected to result in excessive and toxic incorporation of oxidized bases into their DNA.^{6,7} Therefore MTH1 inhibitors might

represent a novel class of anticancer agents with a favorable therapeutic index.^{7–9}

A class of MTH1 inhibitors, as exemplified by **TH287** and cyclopropyl analog **TH588** with nanomolar potency (Fig. 1) against the recombinant enzyme has been recently described, and reported to inhibit cancer cells proliferation at micromolar concentrations.⁹

Here we describe the design and optimization of a novel series of MTH1 inhibitors with sub-nanomolar inhibitory potency, with excellent selectivity (with respect to kinase activity), good physico-chemical properties (including solubility and cell permeability), and excellent microsomal stability. These compounds have been instrumental in allowing us to independently evaluate MTH1 as an oncology target.

An examination of the binding modes of **TH287** and of enzyme substrate 8-O-G (Scheme 1), led us to hypothesize that a 2-amino pyrimidine motif would enable successful engagement of the key interactions made by the guanine motif of the natural substrate. Molecular modeling, using Schrödinger GLIDE XP docking¹⁰ and a docking grid based on the MTH1 protein crystal structure 3ZR0, predicted that the pyrimidine core may participate in π - π interactions with Trp117 and Phe72. The aminopyrimidine would satisfy a hydrogen bonding network with Asp119, Asp120, and Asn33, obviating the need for the additional aminoalkyl substituent present in **TH287**.¹¹ We also noted that the amino alkyl substituent of **TH287** appears to be a metabolic soft spot,⁹ avoiding the need for this substituent might also be advantageous from a metabolic stability standpoint. The 4-hydroxy substituent of the 8-O-G sugar appears to be within H-bonding distance of the backbone carbonyl of Thr8,

^{*} Corresponding author. Tel.: +1 713 794 5263.

E-mail address: apetrocchi@mdanderson.org (A. Petrocchi).

[†] Present address: Cancer Research Technology-Discovery Laboratories, Jonas Webb Building, Babraham Research Campus, Cambridge CB22 3AT, UK.

[‡] Present address: Nurix, 1700 Owens St Suite 290, San Francisco, CA 94158, USA.

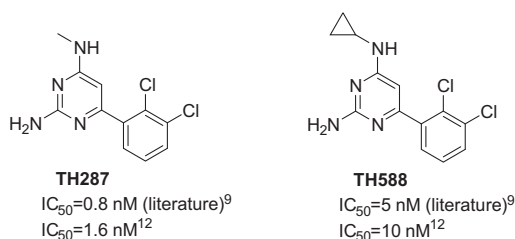


Figure 1. Chemical structure of the MTH1 inhibitors **TH287** and **TH588**.

offering a potential additional interaction to engage. These considerations led us to design compound **1** ($IC_{50} = 4 \mu\text{M}$), which inhibited MTH1 in the single-digit micromolar range (Scheme 1).

The addition of a gem-dimethyl group in the middle of the chain, designed to mitigate the desolvation penalty of the ligand and engage with the lipophilic cavity (exploited by the dichlorophenyl motif of **TH287**), increased the enzymatic potency 26-fold (compound **2**, $IC_{50} = 0.14 \mu\text{M}$).

Removing the terminal hydroxyl group (**3**, Table 1) resulted in increased potency ($IC_{50} = 53$ nM), suggesting that the hydroxyl group is not a net contributor to the in vitro potency of the molecule.

A significant boost in potency came from the substitution of the aminopyrimidine ring with a methyl group in position 5: compound **4** (**IACS-4619**) was identified as a picomolar inhibitor of MTH1 ($IC_{50} = 0.2$ nM). The same outcome was observed for **5** (**IACS-4759** ($IC_{50} = 0.6$ nM)), an analog of compound **2**.

A model of the binding mode of **5** (Fig. 2) docked into MTH1 (derived from PDB: 3ZR0) indicates that the methyl group effectively fills a lipophilic pocket formed by the side-chains of residues Phe27, Phe72, Phe74, Trp117, and Met81. It is possible that the substantial increase in potency results in part from displacement of one or more energetically disfavored water molecules from this region of the protein. Water network analysis using 3D-RISM (as implemented in MOE 2015.10, Chemical Computing Group) was used to examine differences in the positions and energetics of putative water molecules in binding models of compounds **2** and **5**. For compound **2**, there is a poorly bound, or energetically unfavorable, water site adjacent to position 5. This water site is not evident when the analysis is run for compound **5**, suggesting the addition of the methyl group at position 5 has displaced this water molecule. Furthermore, the inclusion of the methyl group might

Table 1
Effect on MTH1 inhibition of substituents at 5 or 6 position of the 2-aminopyrimidine

Entry	Structure	MTH1 IC_{50} (nM) ¹²
3		53 ± 10
4 (IACS-4619)		0.2 ± 0.04
5 (IACS-4759)		0.6 ± 0.16
6		112 ± 21
7		302 ± 44

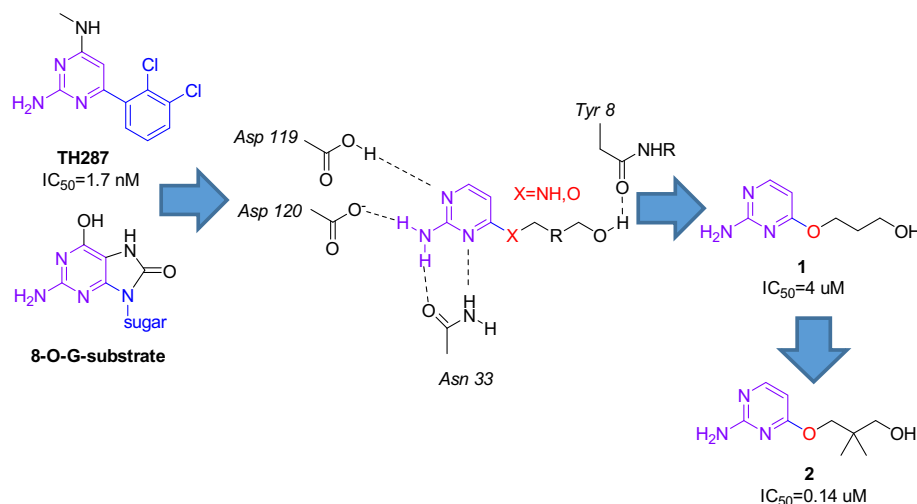
¹²Data are an average of >2 independent determinations.

beneficially impact alignment of the aminopyrimidine with Asp119 and Asp120.¹⁰

Examination of substituents at the adjacent 6-position did not provide the same boost in potency (e.g., compounds **6** ($IC_{50} = 112$ nM) and **7** ($IC_{50} = 302$ nM)). It is apparent that the 5-position offers the optimal trajectory for exploiting this pocket.

Additional exploration of a range of small substituents at the 5-position revealed the methyl to be optimal (Table 2). Chloride **8** ($IC_{50} = 22$ nM) and the methyl ether **9** ($IC_{50} = 10$ nM) conferred no advantage. Fused cyclopentane **10** ($IC_{50} = 4.5$ nM) displayed a 10-fold loss in intrinsic potency compared with **5**.

Intrigued by the influence of the linking atom on preferred conformation of the 4-substituent (and on the pKa of the pyrimidine core), we also explored 4-substituents linked through nitrogen and carbon (Table 3). Replacement of the alkoxy chain with an alkyl amine afforded **11** ($IC_{50} = 2980$ nM), **12** ($IC_{50} = 332$ nM), **13** ($IC_{50} = 120$ nM) and **14** ($IC_{50} = 84$ nM) which confirmed that the amino group was tolerated. The SAR of chain modifications in the diaminopyrimidine series paralleled that of their alkoxy-linked counterparts. Introducing a methyl group in the 5-position



Scheme 1. Structure based design of a novel class of MTH1 inhibitors.

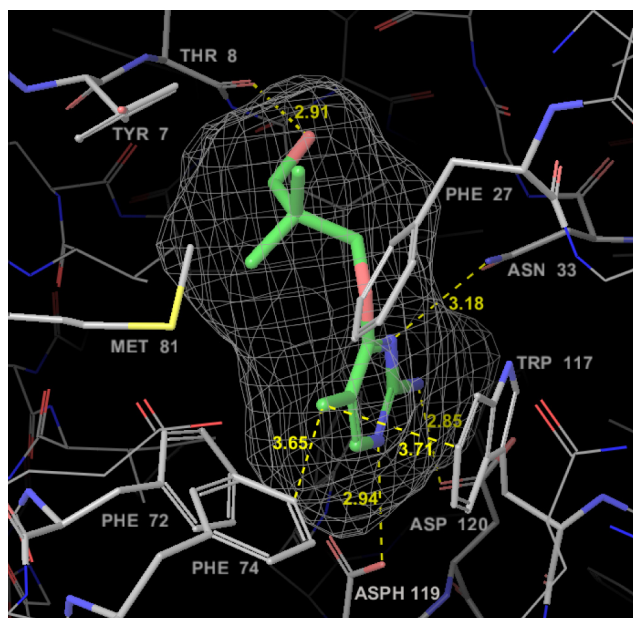


Figure 2. Model of compound **5** docked into the crystal structure of MTH1 (PDB: 3ZRO). Ligand binding surface is represented by gray mesh. Interatomic distances in Å are marked in yellow. The 5-methyl substituent effectively fills a lipophilic pocket formed by the side-chains of residues Phe27, Phe72, Phe74, Trp117, and Met81. The aminopyrimidine engages Asp119, Asp120, and Asn33.

Table 2
Replacing the methyl group at position 5 of the 2-aminopyrimidine

Entry	Structure	MTH1 IC ₅₀ (nM) ¹²
8		22 ± 4
9		10 ± 1
10		4.5 ± 0.9

¹²Data are an average of >2 independent determinations.

generated pyrimidines **15** (IC₅₀ = 3.1 nM) and **16** (IC₅₀ = 0.5 nM) of comparable potency to the alkoxy derivatives. Interestingly, the tertiary amines **17** (IC₅₀ = 0.5 nM) and **18** (IC₅₀ = 0.2 nM) were similarly potent. Furthermore, the introduction of a pyrrolidine, piperidine or a morpholine ring, as alternative replacements for the alkoxy chain, generated compounds with inhibitory activities in the low nanomolar range (data not shown).

A carbon-linked chain in the 4-position of the aminopyrimidine was similarly tolerated (e.g., **19** (IC₅₀ = 1.8 nM)).

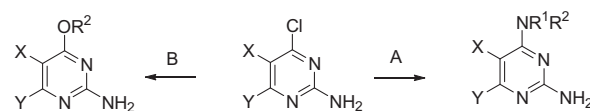
Further SAR exploration of the alkoxy chain indicated significant tolerance for steric bulk and lipophilicity in this region, but conferred no additional advantage to the compounds.

Scheme 2 outlines the synthesis of the aminopyrimidines. Starting with the appropriate 2-amino-4-chloropyrimidine, the alkoxy or the amino moieties were installed via nucleophilic aromatic substitution under basic conditions. The appropriately substituted pyrimidines could also be obtained by reaction of the readily available 2,4-dichloropyrimidines, under conditions A or B and subsequently heating at reflux in ammoniacal ethanol, to

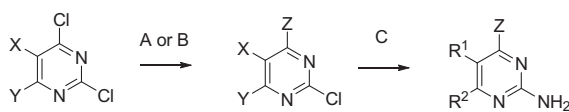
Table 3
Influence of the heteroatom linker at position 4 of the 2-aminopyrimidine

Entry	Structure	MTH1 IC ₅₀ (nM) ¹²
11		2980 ± 497
12		332 ± 42
13		120 ± 20
14		84 ± 17
15		3.1 ± 1.5
16		0.5 ± 0.15
17		0.5 ± 0.12
18		0.2 ± 0.06
19		1.8 ± 0.8

¹²Data are an average of >2 independent determinations.



A = NHR¹R², TEA, EtOH, 150 °C, MW
B = R²OH, NaH, dioxane, 60 °C



C = NH₃ in EtOH (100 °C) or IPA (150 °C)

Scheme 2. General synthetic pathway to afford 2-aminopyrimidine.

install the 2-amino functionality. The route to compound **5** shown in **Scheme 3** was found to be more operationally convenient on a larger scale.

Due to their high enzymatic potency, **4** and **5** were further evaluated (**Table 4**). Compound **5** showed good cell permeability (assessed in a confluent MDCK cell monolayer), solubility (75.6 μM in sodium phosphate buffer (pH = 7.0)), and a high free fraction (46%) in human plasma. It was also found to be stable in rat and human plasma and liver microsomes. In contrast, **4** showed good permeability but high turnover in liver microsomes. The hydroxyl functionality clearly confers significantly improved metabolic stability.

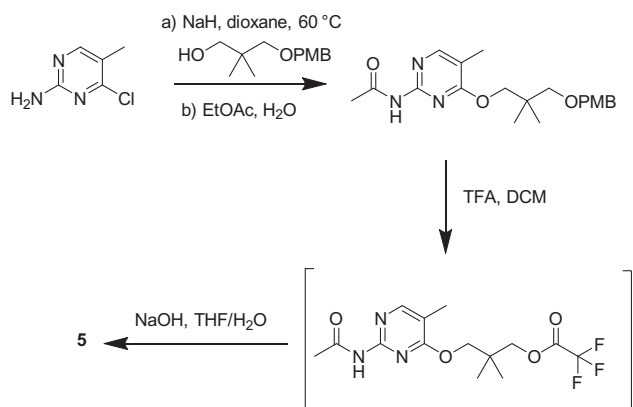
Scheme 3. Synthesis of compound 5.¹³

Table 4
Comparison between **TH287**, **IACS-4759** (compound 5) and **IACS-4619** (compound 4)

Compound	IACS-4619	IACS-4759	TH287
Enzyme IC ₅₀ (nM)	0.2	0.6	1.6
LipE (pIC ₅₀ – cLogD)	6.9	8.0	5.9
Permeability* (10 ⁻⁶ cm/s) (efflux ratio)	37 (0.8)	32 (0.8)	30 (0.8)
Human plasma protein binding (%)	94	54	92 ⁹
Human Cl _{int} (mL min ⁻¹ mg ⁻¹ /T _{1/2} h)	82/0.5	7.5/5.5	54 ⁹ /–
Mouse Cl _{int} (mL min ⁻¹ mg ⁻¹ /T _{1/2} h)	280/0.3	60/1.5	
Plasma stability T _{1/2} h (rat/human)	20/19	86/58	

* Assessed in a confluent monolayer of MDCK cells.

Isothermal Titration Calorimetry (ITC),¹⁴ showed a 1:1 stoichiometry of binding for compound 5 with MTH1, with a significant enthalpic component ($\Delta H = -16.8$ kcal mol⁻¹) to the binding free energy ($\Delta G < -11.2$ kcal mol⁻¹), attesting to the efficiency of the molecular recognition event.

Compound 5 was profiled against a panel of 97 kinases (KinomeEdge panel; DiscoverX™) at 1 μM test concentration. No off-target kinase activity was evident in this panel.

Specific assessment of endogenous MTH1 target engagement in intact cells has proved to be challenging.^{9,15} As a surrogate, U2OS cells were modified to overexpress human MTH1 and treated in culture with increasing concentrations of test compounds. After 1 h treatment, cells were extensively washed, lysed, and the remaining MTH1 activity in the lysate was measured by monitoring the hydrolysis of 8-O-G (Fig. 3). MTH1 activity was found to be significantly inhibited by compounds 4 and 5, indicating that these inhibitors penetrate intact cells, inhibit MTH1, and display a prolonged residency time. The durability of the cellular target engagement, despite the extensive washing protocol, is a testament to the high enthalpy driven MTH1-binding that characterizes these compounds. We did not observe MTH1 inhibition in samples from cells treated with a weaker analog 20¹⁶ (IC₅₀ = 850 nM); with **TH287** and **TH588** some inhibition was observed only at the highest concentrations (data not shown), indicating a potentially faster rate of dissociation from MTH1 in comparison with compounds 4 and 5.

As a control, lysates of MTH1-overexpressing cells were prepared, and then treated with increasing concentrations of compounds. As shown in Figure 4, all the compounds inhibited MTH1 when added directly to the lysates; we observed an excellent correlation between the IC₅₀ measured in the isolated recombinant enzyme assay and the potency in cell lysates.

Having established high potency of MTH1 inhibition, excellent cell penetration, and durability of MTH1 target engagement in the cellular context, we then evaluated the anti-proliferative

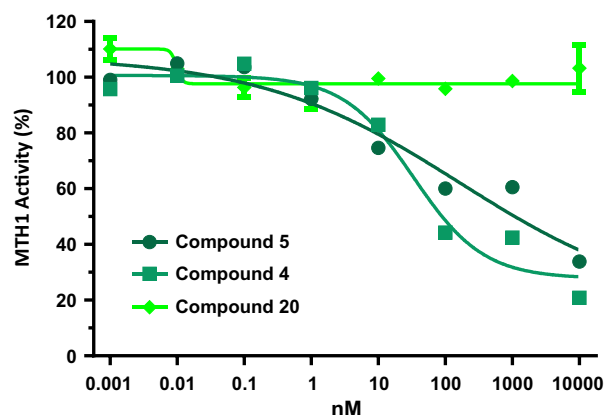


Figure 3. MTH1-overexpressing U2OS cells were treated in culture with increasing concentrations of compound (1 pM–10 μM) for 1 h at 37 °C. Cells were extensively washed, lysed, and 'residual' MTH1 activity was tested with a PpLight™ Pyrophosphate assay.

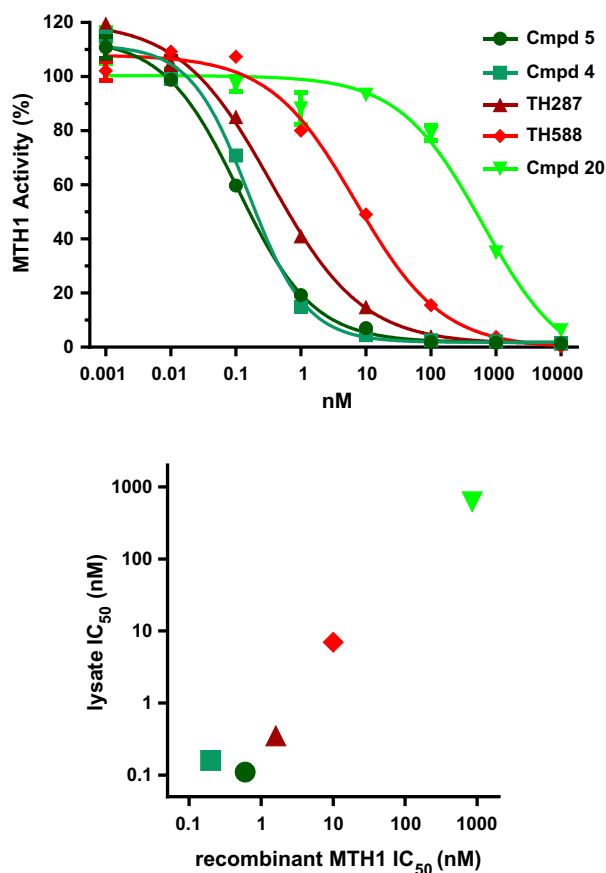


Figure 4. Lysates from MTH1-overexpressing U2OS were treated with increasing concentrations of compound (1 pM–10 μM) and tested for MTH1 activity with a PpLight™ Pyrophosphate assay.

effects of our compounds 4 and 5, in comparison with **TH287** and **TH588**, using a panel of human cancer and normal cell lines.¹⁷ We were not able to observe the expected phenotypic responses for compounds 4 and 5 in any of the tested cells at compound concentrations up to 50 μM, even upon prolonged drug treatments and different assay formats (data not shown). In particular, cell lines characterized by high levels of intrinsic ROS actually tolerated these compounds very well, and no cytotoxicity or antiproliferative

phenotype was apparent. In contrast, we were able to observe a cytotoxic phenotype for **TH287** and **TH588** at micromolar concentrations in these contexts, consistent with the observations previously reported for these compounds.⁹

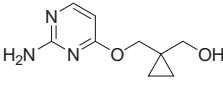
We conclude that selective inhibition of MTH1 by compounds **4** and **5** appears to be insufficient to confer a robust anti-proliferative phenotype in the contexts we have examined thus far. These results also suggest that the mode of action of **TH287** and **TH588** appears to be distinctly different from our compounds, and may involve other factors.

In summary, we have developed a novel series of potent and cell penetrant MTH1 inhibitors with a pharmacological profile that is distinctively different from those already in the public domain. We disclose our compounds as additional tools to further elucidate the biology and pharmacology of MTH1 inhibition.¹⁸

Acknowledgments

We thank Barbara Czako, Maria Emilia Di Francesco, Michael Soth and Wylie Palmer for helpful discussion.

References and notes

- Luo, M.; He, H.; Kelley, M. R.; Georgiadis, M. M. *Antioxid. Redox Signal.* **2010**, *12*, 1247.
- Yoshimura, D.; Sakumi, K.; Ohno, M.; Sakai, Y.; Furuichi, M.; Iwai, S.; Nakabeppu, Y. *J. Biol. Chem.* **2003**, *278*, 37965.
- Nakabeppu, Y.; Tsuchimoto, D.; Furuichi, M.; Sakumi, K. *Free Radical Res.* **2004**, *38*, 423.
- Russo, M. T.; Blasi, M. F.; Chiera, F.; Fortini, P.; Degan, P.; Macpherson, P.; Furuichi, M.; Nakabeppu, Y.; Karran, P.; Aquilina, G.; Bignami, M. *Mol. Cell. Biol.* **2004**, *24*, 465.
- Nakabeppu, Y. *Int. J. Mol. Sci.* **2014**, *15*, 12543.
- Rai, P.; Young, J. J.; Burton, D. G.; Giribaldi, M. G.; Onder, T. T.; Weinberg, R. A. *Oncogene* **2011**, *30*, 1489.
- Helleday, T. *Ann. Oncol.* **2014**, *25*, 1253.
- Huber, K. V.; Salah, E.; Radic, B.; Gridling, M.; Elkins, J. M.; Stukalov, A.; Jemth, A. S.; Göktürk, C.; Sanjiv, K.; Strömberg, K.; Pham, T.; Berglund, U. W.; Colinge, J.; Bennett, K. L.; Loizou, J. I.; Helleday, T.; Knapp, S.; Superti-Furga, G. *Nature* **2014**, *508*, 222.
- Gad, H.; Koolmeister, T.; Jemth, A. S.; Eshtad, S.; Jacques, S. A.; Strom, C. E.; Svensson, L. M.; Schultz, N.; Lundback, T.; Einarsdottir, B. O.; Saleh, A.; Gokturk, C.; Baranczewski, P.; Svensson, R.; Berntsson, R. P.; Gustafsson, R.; Stromberg, K.; Sanjiv, K.; Jacques-Cordonnier, M. C.; Desroses, M.; Gustavsson, A. L.; Olofsson, R.; Johansson, F.; Homan, E. J.; Loseva, O.; Brautigam, L.; Johansson, L.; Hoglund, A.; Hagenkort, A.; Pham, T.; Altun, M.; Gaugaz, F. Z.; Vikingsson, S.; Evers, B.; Henriksson, M.; Vallin, K. S.; Wallner, O. A.; Hammarstrom, L. G.; Wiita, E.; Almlof, I.; Kalderer, C.; Axelsson, H.; Djureinovic, T.; Puigvert, J. C.; Haggblad, M.; Jeppsson, F.; Martens, U.; Lundin, C.; Lundgren, B.; Granelli, I.; Jensen, A. J.; Artursson, P.; Nilsson, J. A.; Stenmark, P.; Scobie, M.; Berglund, U. W.; Helleday, T. *Nature* **2014**, *508*, 215.
- Docking was performed using Glide v 6.3 in extra-precision mode as implemented in Maestro 9.8 (Release 2014-2); Schrödinger, LLC, New York, NY, 2015. [MTH1/8-O-G] PDB 3ZRO; [MTH1/TH588] PDB 4N1U. ACD predicts a 0.5 pK_a increase resulting from introduction of the 5-methyl moiety. The pK_a of the aminopyrimidine of **5** is estimated to lie between 5.8 and 6.1; docking was performed in both the neutral and mono-protonated states and overall docking poses were found to be very similar. Conformational analysis (around ether and amine dihedral) of compound pairs 2/5 and 12/15 using MMFF94 force field show that the protein bound model structures are in the low energy well and very close to global minima in all cases (<2 kcal/mol). As well, the potential energy surface shapes are highly similar for each compound pair. This indicates that the activity improvements are likely not due to differences in conformational state of the molecules. See also: Friesner, R. A.; Banks, J. L.; Murphy, R. B.; Halgren, T. A.; Klicic, J. J.; Mainz, D. T.; Repasky, M. P.; Knoll, E. H.; Shelley, M.; Perry, J. K.; Shaw, D. E.; Francis, P.; Shenkin, P. S. *J. Med. Chem.* **2004**, *47*, 1739; Friesner, R. A.; Murphy, R. B.; Repasky, M. P.; Frye, L. L.; Greenwood, J. R.; Halgren, T. A.; Sanschagrin, P. C.; Mainz, D. T. *J. Med. Chem.* **2006**, *49*, 6177.
- The aryl appendage of **TH287** interacts with Trp117, apparently preventing the aminopyrimidine from penetrating as deeply into the guanine binding site; hence the need for a 6-aminoalkyl substituent to fully engage the guanine binding domain in this class of compounds.
- Compounds were incubated with MTH1 (0.2 nM final concentration), and hydrolysis of 8-oxodGTP (30 μM final concentration) to 8-oxodGMP and pyrophosphate was monitored via a coupled enzyme system using PpiLight™ (Lonza). IC₅₀ values calculated using four-parameter logistic curve fit analysis.
- Synthesis of compound **5**. To a solution of 4-chloro-5-methylpyrimidin-2-amine (500 mg, 3.48 mmol) and 3-((4-methoxybenzyl)oxy)-2,2-dimethylpropan-1-ol (859 mg, 3.83 mmol) in dioxane (10 ml) were added NaH 60% in mineral oil (279 mg, 6.97 mmol) portion wise and the resulting mixture was stirred at 60 °C 18 h. Additional NaH 60% in mineral oil (1.2 equiv) and after 5 h water was slowly added to the mixture. The layers were separated and the aqueous phase was extracted with EtOAc, the combined organic layers were washed with brine, dried over anhydrous Na₂SO₄, filtered and concentrated under reduced pressure. The residue was purified via silica gel chromatography (15–80% EtOAc in hexanes to give *N*-(4-(3-((4-methoxybenzyl)oxy)-2,2-dimethylpropoxy)-5-methylpyrimidin-2-yl)acetamide (896 mg, 2.39 mmol, 69% yield) as a yellow liquid. To a solution of the above acetamide in DCM (4 mL) were added TFA (2 mL) and the resulting mixture was stirred at RT for 2 h. The volatiles were removed under reduced pressure to yield 3-((2-acetamido-5-methylpyrimidin-4-yl)oxy)-2,2-dimethylpropyl 2,2,2-trifluoroacetate, which was directly used as such in the next step. The crude residue was dissolved in MeOH (2 mL), THF (4 mL), water (2 mL) and NaOH (275 mg, 6.87 mmol) was added and the resulting mixture was stirred at 40 °C for 2 h. The mixture was cooled down in an ice bath and pH adjusted to 7 with 6 M HCl (1.5 mL). The volatiles were removed under reduced pressure and the residue was directly purified by mass-triggered preparative HPLC (Mobile phase: A = 0.1% TFA/H₂O, B = 0.1% TFA/MeCN; Gradient: B = 0–40%; 12 min; Column: C18) to give 3-((2-amino-5-methylpyrimidin-4-yl)oxy)-2,2-dimethylpropan-1-ol (425 mg, 2.0 mmol, 88% yield) as a white powder. MS (ES⁺) C₁₀H₁₇N₃O₂ requires: 211, found: 212 [M+H]⁺. ¹H NMR (600 MHz, DMSO-*d*₆) δ ppm 8.14 (br s, 2H), 7.97 (s, 1H), 4.70 (br s, 1H), 4.13 (s, 2H), 3.26 (s, 2H), 1.97 (s, 3H), 0.93 (s, 6H).
- ITC was performed at 25 °C in 100 mM Tris Acetate, 40 mM NaCl, 10 mM Mg Acetate, 0.005% Tween 20, 1 mM Dithiothreitol at pH 7.9. Compound **5** binds with picomolar affinity to MTH1 and therefore the binding affinity and free energy could not be directly determined by ITC as this affinity is beyond the detection limit of the technique. A competition assay was not performed so an upper limit of the affinity (<9 nM) and free energy is provided.
- Leo, E.; Petrocchi, A.; Bardenhagen, J.; Alimova, M.; Shi, X.; Parker, C.; Reyna, N.; Hamilton, M.; Felix, E.; Mazan, A.; Dillon, C.; Mseeh, F.; Marszalek, J. R.; Toniatti, C.; Draetta, G.; Jones, P.; Lewis, R. T. *Poster Presentation: Identification of Potent, Cell Active MTH1 Inhibitors and Their Use in Target Validation Studies*; EORTC: Boston (MA), 2015.
- The structure of compound **20**: 
- U2OS, SaOS2, SW480, HCT116, MDAMB231, HeLa, UOK262, 293T, A549, H460, H358, WI38, BJ, hMEC, MRC5.
- During the preparation of this manuscript we became aware of additional data, independently generated by a group at AstraZeneca using chemical matter that is diverse from ours, but which supports our observations and conclusions. Kevin Foote, personal communication; Kettle, J. G.; Alwan, H.; Bista, M.; Breed, J.; Davies, N. L.; Kay Eckersley, K.; Fillery, S.; Foote, K. M.; Goodwin, L.; Jones, D. R.; Käck, H.; Lau, A.; Nissink, J. W. M.; Read, J.; Scott, J. S.; Taylor, B.; Walker, G.; Wissler, L.; Wylot, M. *J. Med. Chem.* manuscript submitted.